GEOSCIENTIFIC REPORT

GR2006-1

# Geology of the Thompson Bay–Persian Lake area, North Arm, Athapapuskow Lake, Manitoba (NTS 63K12NE)

By
D.E. Prouse

Manitoba

Geoscientific Report GR2006-1

# Geology of the Thompson Bay–Persian Lake area, North Arm, Athapapuskow Lake, Manitoba (NTS 63K12NE)

by D.E. Prouse

Winnipeg, 2006

When using information from this publication in other publications or presentations, due acknowledgment should be given to the Manitoba Geological Survey. The following reference format is recommended:

Prouse, D.E. 2006: Geology of the Thompson Bay–Persian Lake area, North Arm, Athapapuskow Lake, Manitoba (NTS 63K12NE); Manitoba Industry, Economic Development and Mines, Manitoba Geological Survey, Geoscientific Report GR2006-1, 17 p.

**NTS grid:** 63K12NE

**Keywords:** Manitoba, Trans-Hudson Orogen, Flin Flon Belt, Amisk collage, Athapapuskow Lake, Persian Lake, island arcs, calc-alkalic composition, geochemistry, mid-ocean ridge basalts, Hotstone occurrence, massive sulphide deposits, volcanism

**Published by:**
Manitoba Industry, Economic Development and Mines
Manitoba Geological Survey
360–1395 Ellice Avenue
Winnipeg, Manitoba
R3G 3P2 Canada

| | |
|---|---|
| Telephone: | (800) 223-5215 (General Enquiry) |
| | (204) 945-4154 (Publication Sales) |
| Fax: | (204) 945-8427 |
| E-mail: | minesinfo@gov.mb.ca |
| Website: | http://www.gov.mb.ca/iedm/mrd/ |

**Cover illustration:** White aphyric rhyolite tongues enveloped in gritty brown hyaloclastite, exposed 350 m southeast of the Hotstone occurrence at Thompson Bay, Athapapuskow Lake.

## ABSTRACT

Field mapping of the area extending from the east shore of the North Arm of Athapapuskow Lake east to the Persian Lake area has revealed a thick bimodal sequence of mafic and felsic volcanic flows intruded by synvolcanic dikes and late diabase and granodiorite intrusions. The western portion of the map area (near Athapapuskow Lake) is dominated by well-preserved mafic and felsic volcanic flows that trend northeast. A large diabase dike and a late granodiorite body intrude mafic and felsic flows in the central portion of the map area. Gabbro and diorite intrude predominantly mafic flows in the north-central and northeastern parts of the map area. Rocks west of Persian Lake consist of massive felsic and intermediate flows and intrusions with lesser amounts of mafic material. These rocks are essentially devoid of any volcanic textures, possibly a result of proximity to the large intrusive body east of Persian Lake. Late diabase and gabbroic dikes cut the volcanic rocks in the Persian Lake area.

Volcanic flows in the western portion of the map area are overprinted by a north-northeast-trending schistosity. Rock units near Persian Lake have a northerly trend that becomes northeasterly farther to the west. Schistosities are often poorly preserved and are overprinted with a prevalent north-northeast-trending shear foliation. Rock units throughout the map area have been subjected to significant stress that produced faults in the North Arm area of Athapapuskow Lake and shears and faults in the central and Persian Lake areas. The bimodal stratigraphic package faces southeast except in the northwest corner of the map area (east of the Hotstone mineral occurrence), where pillowed basaltic andesite faces north-northwest. The axial plane of a northeast-striking fold structure is assumed to occur in the area of the small lakes in the northwestern part of the map area. Lack of good exposure prevented this feature from being pinpointed on the ground.

Major and trace element geochemistry of Thompson Bay–Persian Lake basaltic andesite indicates a volcanic arc (VAB) origin with calcalkaline or high-K affinity (e.g., selective enrichment of Th and, to a lesser extent, Ce relative to other elements, significant negative Nb anomaly and depletion of Ti and Y). Rhyolite is also calcalkaline (e.g., small negative Eu anomaly and moderate $[La/Yb]_N$ ratio).

Petrographic thin-section analysis reveals that alteration consisting of actinolite, chlorite, epidote and sericite is prevalent throughout the map area. Sulphide mineralization is commonly associated with shears and faults throughout the map area. Thin units of poorly exposed oxide- and sulphide-facies iron formations are present in the Persian Lake and central parts of the map area. Rhyolitic rocks have been subjected to iron-magnesium alteration in the central part of the map area and west of Persian Lake.

## TABLE OF CONTENTS



## TABLES



## FIGURES

**MAP**

## Introduction

Geological mapping at 1:5000 scale commenced in 1994 in the Thompson Bay area of Athapapuskow Lake (Gale et al., 1994) to better define felsic volcanic flows in a previously undivided mafic volcanic sequence that had initially been mapped at 1:63 360 scale (1 inch to 1 mile) by Buckham (1944). The 1:5000 scale mapping project was expanded from Athapapuskow Lake east to the Persian Lake area in order to include felsic volcanic rocks that had been reported in the vicinity of the Hotstone mineral occurrence by Gale and Eccles (1992). Mapping was conducted using cut gridlines in the Thompson Bay area and 1:5000 scale airphotos in the balance of the area.

The Thompson Bay–Persian Lake map area is located in the Flin Flon Belt of the Trans-Hudson Orogen (Figures 1–3). It is part of the Bakers Narrows Block (Figure 3) of Bailes and Syme (1989). The northern portion of the map area is included in simplified form in a map of the Baker Patton Complex by Gale and Dabek (2002). The area is bounded to the west by the North Arm Fault, to the north by the South Baker Patton Fault and to the east by the granodiorite intrusion just east of Persian Lake (Figure 4). Mapping extended south to the Sharpe Bay area. Summary reports of results of field mapping programs are described in Prouse (1995, 1996) and Gale et al. (1994).

## Regional setting

The map area is located in the central Flin Flon Belt (Figure 3), which comprises a number of volcanosedimentary assemblages that form part of a Paleoproterozoic accretionary complex (1.92–1.88 Ga Amisk collage of Lucas et al., 1996). The Flin Flon Belt is bounded to the north by metasedimentary gneiss of the Kisseynew Domain and to the south by flat-lying Paleozoic rocks of the Western Interior Platform (Figure 2).

Tectonostratigraphic assemblages within the Amisk collage include juvenile arc, juvenile ocean floor, ocean plateau–ocean island basalt, evolved arc and Archean crustal slices (Figure 3). The distinct assemblages in the central part of the Flin Flon Belt were juxtaposed during 1.88–1.87 Ga intraoceanic

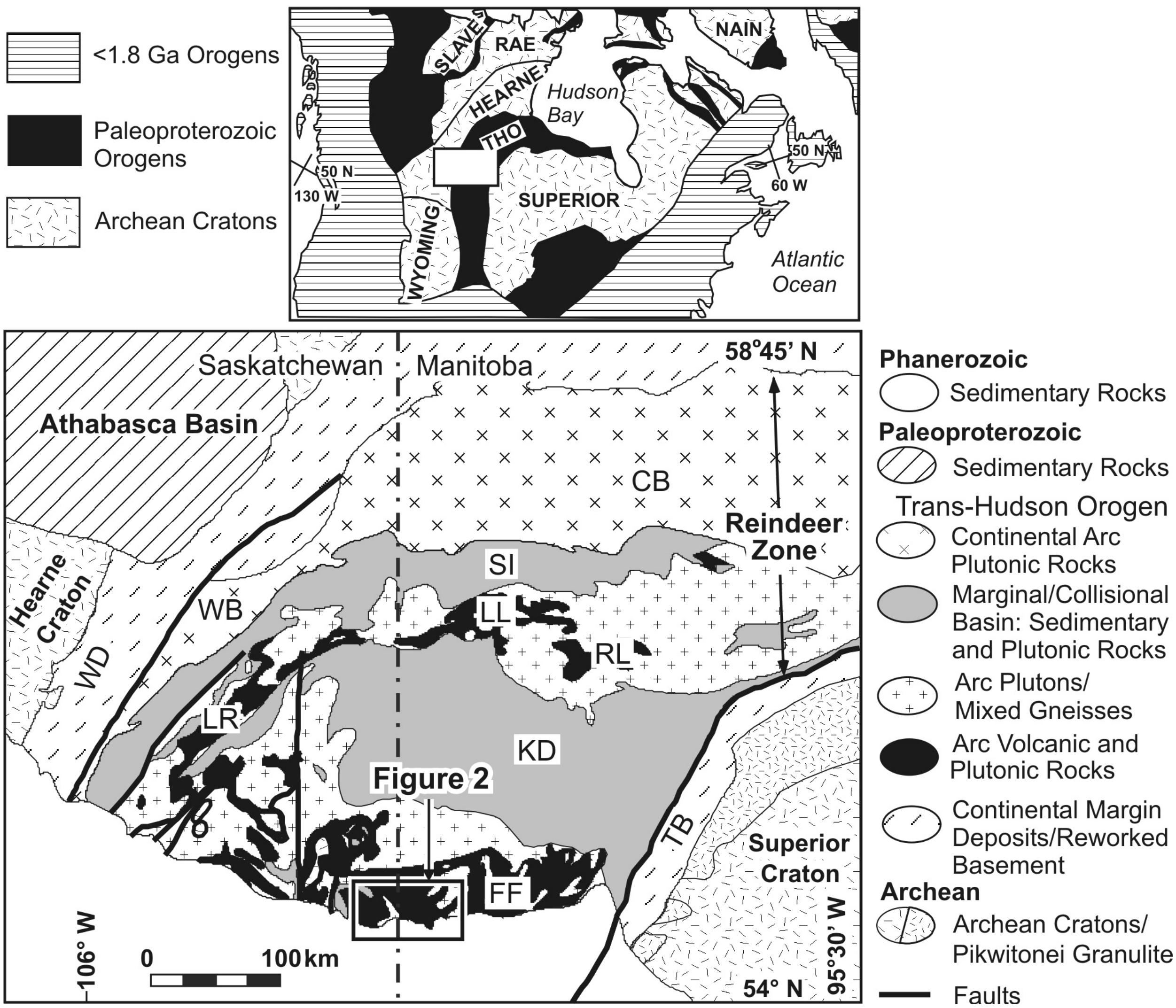


***Figure 1:** Tectonic elements of the Trans-Hudson Orogen in northern Manitoba and Saskatchewan (*after *Hoffman, 1988). Abbreviations: CB, Chipewyan Batholith; FF, Flin Flon Belt; LL, Lynn Lake Belt; LR, La Ronge Belt; RL, Rusty Lake Belt; SI, Southern Indian Belt; TB, Thompson Belt; WB, Wathaman Batholith; WD, Wollaston Domain.*

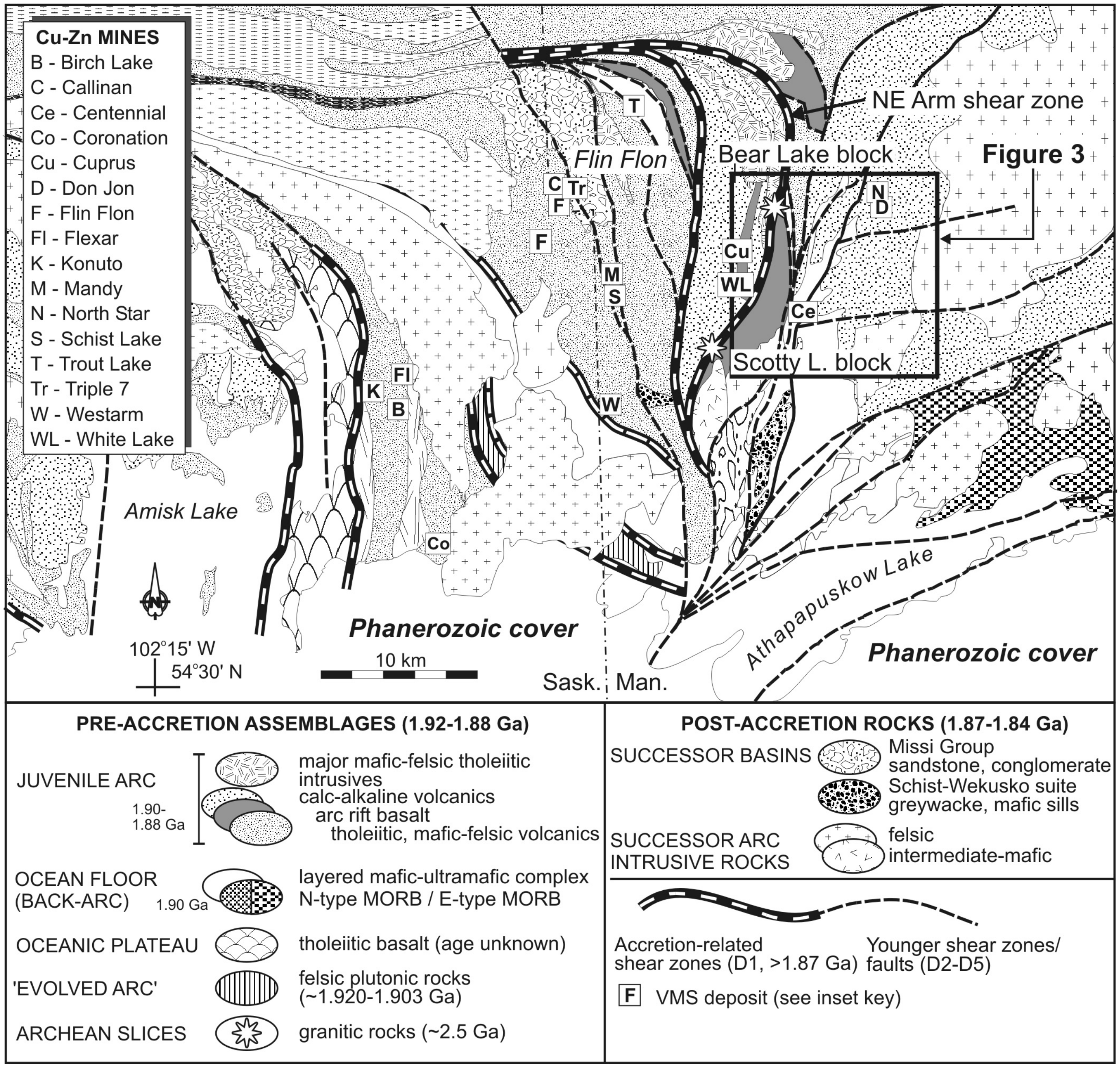


***Figure 2:** Tectonic assemblages of the central Flin Flon Belt, showing the location of the Thompson Bay–Persian Lake map area (*modified from *Syme et al., 1996).*

accretion, prior to the emplacement of granitoid plutons (Syme et al., 1996). The Flin Flon Belt contains six geographically separate juvenile arc assemblages, each of which is 20–50 km across (Hanson Lake, West Amisk, Birch Lake, Flin Flon, Fourmile Island and Snow Lake). These are separated by major faults, ocean floor rocks, Burntwood Group turbidites, plutons or a combination of these rock types (Lucas et al., 1996). The Amisk collage formed the basement during 1.87–1.83 Ga post-accretion magmatism, expressed as voluminous calcalkaline plutons and rarely preserved calcalkaline to alkaline volcanic rocks. Younger sedimentary and volcanic rocks (e.g., Missi Group) may represent depositional basins that formed contemporaneously with postaccretion arc magmatism and deformation (Lucas et al., 1996).

The Flin Flon arc assemblage contains mostly mafic volcanic rocks that were deposited in a subaqueous environment, with some pyroclastic rocks possibly erupted in a very shallow marine or subaerial setting (Bailes and Syme, 1989; Dolozi and Ayres, 1991). Basalt and basaltic andesite flows dominate the assemblage and belong mainly to tholeiitic and calcalkaline suites (Stern et al., 1995). Pillow fragment breccias and mafic pyroclastic rocks are locally abundant, forming units a few metres to hundreds of metres thick. Rhyolite flows and associated felsic volcaniclastic rocks occur sporadically throughout predominantly mafic successions. The volcanic sequences represent a proximal facies with respect to source

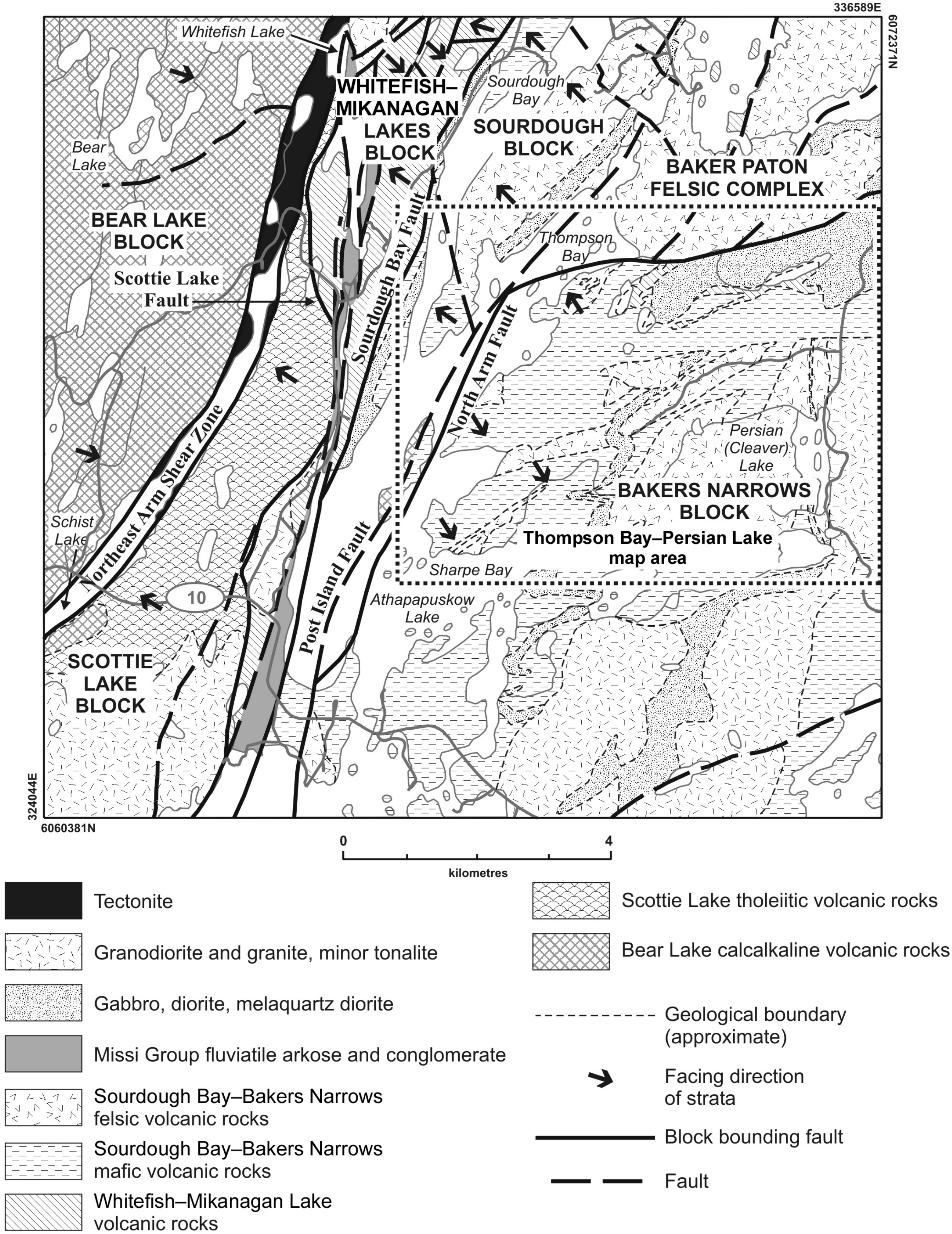


***Figure 3:*** *Location of the Thompson Bay–Persian Lake map area with respect to major structural blocks and tectonostratigraphic assemblages exposed on northern Athapapuskow Lake.*

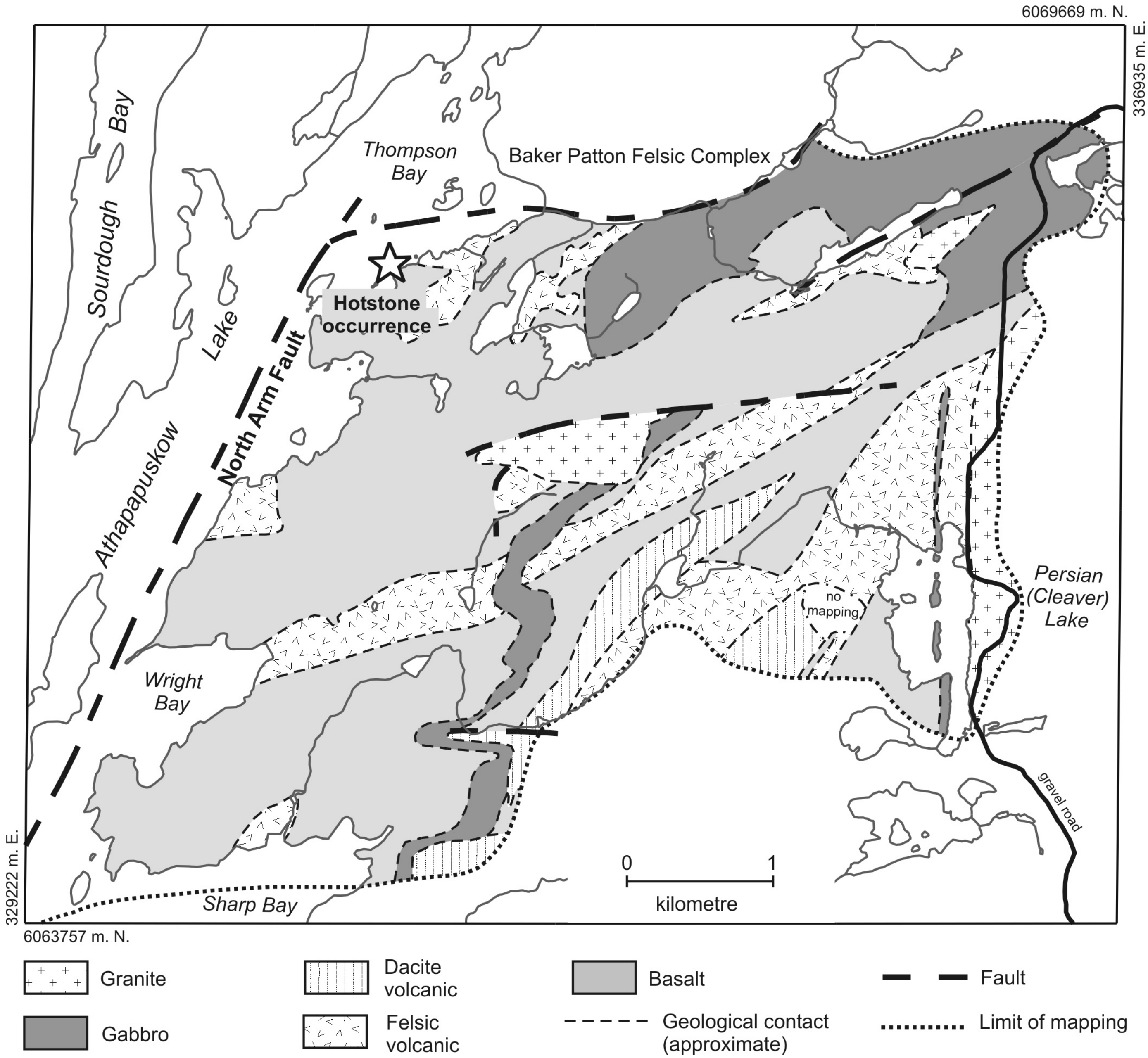


***Figure 4:*** *Simplified geology of the map area, with the Hotstone occurrence located near the southeast shore of Thompson Bay, Athapapuskow Lake.*

vents, as shown by the thickness of the volcanic components and scarcity of sedimentary interbeds. Synvolcanic intrusive rocks are common and include a wide variety of rock types, interfingering relationships, lenticular units and abrupt facies variations (Syme et al., 1996).

A system of north- to northeast-trending, vertical, brittle to ductile faults and shear zones exerts fundamental control on the distribution of rock types in the Flin Flon arc assemblage (Figures 3 and 4). Regional metamorphic grade at Flin Flon increases northward, toward the Kisseynew metasedimentary gneiss belt, from prehnite-pumpellyite through greenschist to amphibolite facies. Most rocks have greenschist-facies mineral assemblages (actinolite-chlorite-quartz-epidote-plagioclase; Stern et al., 1995).

## Unit descriptions

### *Basalt, basaltic andesite (unit 1)*

Mafic volcanic rocks constitute approximately 60–70% of the supracrustal rocks in the Thompson Bay–Persian Lake area. Along the east shore of Thompson Bay, a large proportion of the mafic rocks is composed of well-preserved volcaniclastic material. Pillowed and massive flows constitute a small proportion by volume in this area. Massive mafic volcanic rocks of uncertain genesis are common farther to the east in the vicinity of the intrusions. In this area, rocks are typically strongly recrystallized, with primary textures at least partially obliterated.

Compositionally, there are at least three types of mafic flows in the map area: 1) plagioclase phyric, 2) pyroxene phyric, and 3) aphyric. Due to intense lichen and moss cover, however, it was not possible to properly separate the mafic volcanic rocks on the basis of phenocryst content.

**Massive flows (unit 1a)**

Massive mafic flows are medium green to light brown weathering and medium to dark green on fresh surfaces. Overall, massive flows are aphyric in the northern portion of the map area and aphyric to weakly plagioclase or pyroxene phyric in the south. Massive flows consist of an aphanitic aggregate of plagioclase, amphibole±pyroxene, chlorite-actinolite and trace to 2% pyrite. The more basaltic variety of flows contains a higher proportion of chlorite and amphibole than the andesitic variety, which is more prominent in the north-central part of the map area.

Massive flows in the vicinity of Athapapuskow Lake (better preserved) typically contain 1–3% vesicles that average 1–2 mm in diameter and range up to 3–7 mm and rarely up to 10–20 mm in some flows. Amygdules filled with quartz, carbonate, alkali feldspar and, less commonly, epidote together constitute 2–4% of the rock.

Massive mafic flows in the central part of the map area and west of Persian Lake are weakly foliated to nonfoliated and hard, and often contain abundant white to pale green silica and/or epidote veins or veinlets 1–3 mm in thickness. These hard mafic flows contain irregular fracture cleavage or joint sets. Occasionally, amygdaloidal zones are preserved to some degree. Especially in the north-central part of the area, massive mafic flows have zones that have a microgabbroic texture, suggesting that some may be synvolcanic intrusions or fine-grained mafic dikes cutting basaltic andesite flows.

**Lapilli tuff (unit 1b)**

Mafic lapilli tuff is commonly associated with flow breccia and occasionally occurs as discrete layers within massive flow sequences. Lapilli tuff consists of a medium to dark green matrix with subangular to subrounded buff to light green fragments. The unit is matrix supported to weakly fragment supported, and commonly weakly to moderately vesicular and/or amygdaloidal. Vesicles are normally in the 2 mm diameter range, but some tuff units in the Thompson Bay area contain vesicles up to 25 mm diameter. Vesicles are rimmed or filled with quartz, carbonate, alkali feldspar, epidote or amphibole. In some sequences, highly vesicular tuff occurs as discrete layers, a few metres thick, between flow breccia and massive flow sections. Thicker sequences of lapilli tuff contain 2–3 m thick layers of vesicular flow breccia.

**Flow breccia, pillow fragment breccia (unit 1c)**

Basaltic-andesite flow breccia and pillow fragment breccia form a large portion of the exposed rocks in the western portion of the map area. Breccia textures vary from subangular to amoeboid blocks to tuff-breccia, sometimes within the same flow sequence. Breccia fragments weather buff-brown to dark grey and vary in size from <1 cm to tens of centimetres in diameter (Figure 5). Fragment content varies from about 50 to 70%. Breccia units near Athapapuskow Lake are commonly matrix supported, whereas those farther to the east are fragment to weakly matrix supported. In the northwestern part of the map area, mafic breccia fragments are commonly silicified to some extent. Vesicularity and amygdule content are quite variable. Fragment vesicularity ranges from <1 to 20%. Amygdule content ranges from <1 to 25%, with 5–10% being common. The amygdules, ranging from <1 to 2 cm in diameter, are filled with variable amounts of quartz, carbonate, epidote or alkali feldspar. The hyaloclastite matrix is notably darker coloured, weathers medium to dark green and is composed of a mixture of lapilli, tuff and quartz phenocrysts in a fine-grained groundmass of plagioclase, pyroxene and amphibole±chlorite-actinolite.

**Pillowed flow (unit 1d)**

Well-preserved pillowed flow units are sparsely exposed in the western part of the map area, primarily in the Hotstone


***Figure 5:*** *Basaltic andesite flow breccia–pillow fragment breccia with chloritic matrix and partially silicified fragments, east shore of Thompson Bay.*

occurrence and Wright Bay areas. In the Hotstone occurrence area, pillowed flows vary from 20 m thick with amoeboid megapillows up to 6 m in length to approximately 5 m thick with flattened pillows averaging 0.5 m in length. The amoeboid pillowed unit is light green on weathered surfaces and highly vesicular (up to 30% vesicles), with vesicles to 5 cm diameter commonly filled with quartz and/or alkali feldspar. This thick amoeboid pillowed flow unit has a topping sense toward the north-northwest. The thinner flattened pillowed flow unit, located south of the Hotstone occurrence, is 5% plagioclase-feldspar phyric and moderately vesicular, with 2–7 mm vesicles and 2–3% 1–3 mm alkali feldspar– and epidote-filled amygdules. The pillows, which are adjacent to a shear zone, have a flattening ratio of approximately 10:1. This unit faces east-southeast.

The areas north and northeast of Wright Bay contain a number of poorly to well-preserved mafic pillowed flows. These pillowed flow units are buff brown to medium green on weathered surfaces and have exposed thicknesses ranging from 10 to 30 m. Pillows are rounded to irregular and 0.5 to 1.5 m long. The flows vary from aphyric to feldspar phyric and occasionally pyroxene±feldspar phyric. They are commonly moderately to highly vesicular, with 10–20% vesicles 1–5 mm in diameter, and less frequently amygdaloidal, with up to 15–20% alkali feldspar– and epidote-filled amygdules 2–8 mm in diameter. All pillowed flow units in the Wright Bay area face southeast.

### *Rhyolite (units 2, 3 and 4)*

Several varieties of rhyolite occur throughout the Thompson Bay–Persian Lake map area, interbedded with mafic flows (Figure 4). Detailed mapping of these rhyolites has categorized them by phenocryst type into quartz phyric (unit 2), quartz-feldspar phyric (unit 3) and aphyric (unit 4) types.

#### Quartz-phyric rhyolite (unit 2)

Quartz-phyric rhyolite is proportionally the most abundant type of rhyolite in the map area. As with all other volcanic rocks in the area, primary textures are better preserved in those rocks that outcrop near Athapapuskow Lake.

Close to Athapapuskow Lake, quartz-phyric rhyolite flows are typically composed of a massive base with or without a flow-lobe section with accompanying hyaloclastite. This is topped by a relatively thin flow-breccia section that is commonly a few metres in thickness. Massive flows have a beige-buff weathered surface and are light green-grey on fresh surface. The unit contains from <1 to 3% (rarely 4% or greater), angular to subangular, 1–3 mm, white to smoky grey quartz phenocrysts in a fine-grained groundmass of quartz, plagioclase and minor hornblende±chlorite.

Quartz-phyric rhyolite flow-lobe sections vary from a few metres to 15–20 m in thickness. Individual lobes vary from <1 to 10 m in length and are 0.5–3 m wide (Figure 6). The length:width ratio is approximately 3:1. Lobes are commonly partially to completely enveloped by a gritty textured hyaloclastite composed of granules, shards and fragments 3–5 mm in diameter. Typically, the hyaloclastite is moderately to well foliated, vesicular and altered to chlorite±carbonate±silica. Lobes often contain well-developed fracture cleavage, as well as quartz-filled tension gashes. Rhyolite flow sequences containing lobes occur in the southwestern (Wright Bay and Sharpe Bay), west-central and north-central portions of the map area. This is contrary to the observation by Bailes and Syme (1989) that the Bakers Narrows Block rhyolite flow sequences are devoid of rhyolite lobes and pods. Since Bailes and Syme found no rhyolite lobes within the Bakers Narrows rhyolite flows, they considered their flow morphology to be different than those at Solodiuk Lake and Grassy Narrows. Detailed mapping of the Thompson Bay–Persian Lake area does not support this hypothesis. Bailes and Syme (1989) suggested that differences in felsic flow morphology in the Bakers Narrows Block may reflect a difference in depth of emplacement, and the lack of highly vesicular material associated with felsic flows suggests a greater depth of subaqueous emplacement. The author supports this theory, since the majority of felsic flows examined contained very little pumiceous material.

***Figure 6:*** *Large rhyolite lobe enveloped by vesicular hyaloclastite, north of Wright Bay, scale in centimetres.*

Quartz-phyric rhyolite flow breccia constitutes a small portion of the flow when it occurs with massive flow and lobes. This is interpreted to be a function of viscosity of the lava. The breccia consists of angular to subrounded fragments ranging from a few centimetres to 50 cm in diameter. The breccia is usually matrix supported with rare fragment-supported zones. Fragments contain 1–3% angular to subrounded, white to smoky grey quartz phenocrysts 1–5 mm in diameter. Fragments often contain 2–5% vesicles or quartz-filled amygdules. The matrix commonly contains a lesser amount of vesicles and/or amygdules.

Quartz-phyric rhyolite tuff is rare and occurs primarily in the vicinity of the small lakes in the north-central part of the map area. They are white to buff on weathered surfaces and light to medium grey on fresh surfaces. Quartz phenocryst content varies from <1 to 4% (generally 1–2%), and the phenocrysts are 2–3 mm in diameter. Fragments in the tuff are generally <1 cm in diameter, subangular and matrix supported. The tuff layers are thin, ranging from a few to tens of centimetres overlying massive flow sections, and they grade into flow breccia layers 5–10 m in thickness. The unit is commonly massive and weakly vesicular. Some tuffaceous layers contain chlorite patches or stringers. The stringers sometimes contain a solution cleavage concordant to the $S_2$ foliation.

#### Quartz-feldspar–phyric rhyolite (unit 3)

Quartz-feldspar–phyric rhyolite outcrops sporadically on the shore of Thompson Bay and in the northern portion of the map area, where it is intercalated with massive basaltic andesite. This light grey unit comprises massive flows, lobes and lapilli tuff. The unit contains <1 to 2% grey, subangular quartz phenocrysts and 1 to 4% white to pinkish, anhedral feldspar. Typically, the massive flow and lapilli tuff sections are slightly to moderately vesicular. The matrix of lapilli tuff and hyaloclastite sections of lobes are commonly partly altered to chlorite.

The unit also occurs as narrow (2–5 m thick) dikes and sills that intrude mafic flows and gabbro/diorite intrusions in the north-central part of the map area. These dikes/sills have a north-northeast trend.

Near the shore of Thompson Bay, quartz-feldspar–phyric rhyolite is also intercalated with basaltic andesite. In this area, quartz-feldspar–phyric rhyolite is composed of massive flow, flow breccia and flow lobes. It has a beige-grey weathered colour and is dark grey-green on fresh surfaces. A portion of the massive flow contains quartz-filled amygdules, silicified fragments and networks of silica veinlets, indicative of hydrothermal seawater alteration. Flow breccia is composed of 70–80% subrounded fragments, up to 50 cm diameter, supported by a fine-grained matrix containing up to 30% chlorite and epidote±carbonate, and 3–5% vesicles 1–2 mm in diameter.

#### Aphyric rhyolite (unit 4)

Aphyric rhyolite with preserved primary extrusive textures is rare and confined to the area at the north end of Thompson Bay, near the Hotstone occurrence. Unit 4 rhyolite is medium green on weathered surfaces and beige-pink on fresh surfaces. It is mainly composed of massive flows, flow breccia and lapilli tuff with subangular fragments; they are slightly to moderately vesicular. Distinctive chalk-white, aphyric rhyolite tongues, approximately 5 m long by 0.5 m wide and enclosed in medium brown hyaloclastite, are exposed in small outcrops 350 m southeast of the Hotstone occurrence. The hyaloclastite appears to have been subjected to iron-magnesium alteration in the coarser grained sections. Locally, aphyric rhyolite may contain up to 3% subangular metasomatic feldspar up to 2 mm in diameter.

In the central and Persian Lake parts of the area, aphyric rhyolite is generally massive and takes the form of dikes, sheets and irregularly shaped bodies. The unit is beige to light grey on weathered surfaces and medium grey on fresh surfaces. Near Persian Lake, aphyric rhyolite is intercalated with quartz-phyric rhyolite, intermediate (dacitic) dikes, fine-grained mafic dikes and massive basaltic andesite. Aphyric rhyolite, exposed on islands and the shoreline of Persian Lake, is strongly sheared and contains chlorite stringers ± pyrite. Rare exposures of aphyric rhyolite breccia in the central and northeastern parts of the map area contain 5–10 cm fragments and blocks that are matrix supported. Fragments and/or matrix are commonly altered to chlorite or epidote. Poor exposure does not allow distinction between actual flow-breccia units and late zones of deformation.

### *Dacite (unit 5)*

Dacite flows and dikes occur in the Wright Bay and Sharpe Bay areas. North of Wright Bay, a 20–40 m thick dacite tuff-breccia unit occurs between felsic and mafic flows. The unit has a light brown weathered colour, is aphyric to 5% quartz phyric and contains lapilli-sized fragments and the occasional breccia fragment up to 0.6 m in length. The matrix is weakly vesicular. Fragments are moderately vesicular and subrounded, and have a more felsic composition than the matrix. Dacite bodies in the Sharpe Bay area are poorly exposed. Where observed, they take the form of 5–10 m thick, massive, quartz-phyric dikes that intrude massive basaltic andesite flows.

An inferred 300 m thick section of dacite flows occurs in the central part of the map area (Figure 4). The flows are generally massive, with a few thin (0.5–0.75 m) tuff-breccia layers containing subrounded fragments. The unit has a light green-grey weathered colour, is 1–7% alkali-feldspar phyric and/or contains up to 2% quartz phenocrysts. The phenocrysts are set in a fine-grained groundmass of quartz, feldspar, amphibole and chlorite. This dacite unit is intercalated with massive mafic and felsic flows.

Dacite in the Persian Lake area is massive, fine grained and strongly recrystallized, exhibiting no volcanic textures. It forms sills or dike-like bodies ranging in thickness from a few centimetres to tens of metres. It is medium grey to brownish on weathered surfaces and commonly contains 1–3% anhedral, cream-white, 1–3 mm alkali feldspar phenocrysts in a matrix of feldspar and quartz with a variable amount (5–20%) of biotite and/or hornblende, which sometimes imparts a gneissic or laminated texture. The dacite postdates rhyolite and predates fine-grained mafic (doleritic) dikes in the area west of Persian Lake.

## *Rhyolite intrusions (unit 6)*

### Quartz±feldspar–phyric and aphyric rhyolite dikes (unit 6a)

Massive quartz±feldspar–phyric and aphyric dikes occur throughout the map area. They are typically light grey to buff on weathered surfaces and medium grey on fresh surfaces. Quartz phenocryst content varies from nil to 4%; they are usually 0.5–3 mm in diameter, angular to subangular and whitish to smoky grey in colour. Feldspar phenocrysts, when present, consist of 1–4% subhedral, white potassium feldspar 1–3 mm in diameter. The observed thickness of dikes varies from approximately 1 to 15 m. The unit is typically massive, although rhyolite dikes exposed in the vicinity of late mafic intrusions (diabase dikes) have a moderate to weak foliation. An altered (sheared?) rhyolite dike in the south-central part of the area contains 2–3 mm wide quartz-carbonate and chlorite veins/veinlets.

### Hypabyssal rhyolite intrusion and dikes (unit 6b)

Rhyolite belonging to unit 6b intrudes massive aphyric and plagioclase-pyroxene–phyric basaltic andesite east of Sharpe Bay. The rhyolite intrusion is light grey to beige on weathered surfaces and medium grey on fresh surfaces. It contains 1% quartz phenocrysts, 3–4% metasomatic feldspar and commonly up to 1% magnetite set in a fine-grained groundmass of quartz, potassium feldspar, plagioclase and minor biotite. The unit contains 1–10 m thick (or greater) hornfelsed xenoliths and irregularly shaped masses of basaltic andesite. The mafic xenoliths contain local veinlets and clots of silica. The western margin of the intrusion consists of a repetitive sequence of rhyolite dikes, ranging from <1 m to tens of metres in thickness, separated by basaltic andesite sheets and blocks. The steeply dipping rhyolite dikes have a prominent 40–60° trend. A distinctive quartz porphyry (unit 6c) occurs near the western contact of the rhyolite dikes.

To the east, the mafic xenolith content decreases and rhyolite intrusive material becomes thicker. Narrow (5–10 m) diabase dikes intrude the rhyolite intrusive unit and are generally concordant with dikes and xenolith layers. Massive basaltic andesite on the northern and eastern margins of the rhyolite intrusion contain rhyolite dikes and quartz-carbonate– and potassium-feldspar–rich zones.

### Quartz porphyry (unit 6c)

A large intrusion of quartz porphyry cuts aphyric rhyolite flows and basaltic andesite approximately 500 m southeast of the Hotstone occurrence. The intrusion contains varying amounts (up to 30%) of whitish grey quartz phenocrysts, up to 7 mm in diameter, in a beige–light green siliceous matrix. Petrographic analysis indicates that the groundmass consists of 30% subangular, 0.1–0.5 mm quartz grains as aggregates and encompassing relict alkali feldspar(?) that is completely altered to sericite and carbonate. The unit is generally massive but contains numerous veins and stringers of quartz and alkali feldspar. Smaller exposures of the porphyry unit take the form of dikes that intrude aphyric rhyolite. The quartz porphyry dikes contain a lesser amount (5–10%) of quartz phenocrysts.

## *Metasedimentary rocks (unit 7)*

Small exposures of iron formation (unit 7) are the only metasedimentary rocks encountered in the map area. They are intercalated with the volcanic rocks and, for this reason, are thought to be the same age as the volcanic rocks and to represent a hiatus in volcanism during which chemical sedimentation took place. Most of the iron formation was found within or adjacent to felsic to intermediate flows.

### Oxide-facies iron formation (unit 7a)

Exposures of oxide-facies iron formation are rare within the map area. The only good exposure encountered is located 800 m west of the north end of Persian Lake. At this location, a tight, S-asymmetric, isoclinally folded layer of chert-magnetite iron formation occurs within massive basaltic andesite. The folded layer measures approximately 4.5 m thick and consists of millimetre- to centimetre-thick alternating bands of chert and magnetite. The axial plane of the minor fold strikes 271°, dips 60°N and plunges east.

### Sulphide-facies iron formation (unit 7b)

Small exposures of sulphide-facies iron formation occur in the Sharpe Bay and south-central parts of the map area. They are primarily associated with aphyric and quartz-phyric rhyolite and dacite bodies situated within thick basaltic andesite flow sequences. Iron formation units examined are on the order of a few metres thick and consist of alternating bands or zones of quartz, chert, magnetite and argillite, plus disseminations, seams or blebs of pyrite. Up to 15% white pyrite stringers ± arsenopyrite was noted at one location in the south-central part of the area. Sulphide-facies iron formations are frequently sheared and occasionally folded, the layering outlining minor S-folds with a moderate easterly plunge.

## *Mafic to intermediate intrusions (unit 8)*

A number of mafic to intermediate intrusive rock types are found within the map area. The genetic association of these intrusions and their mutual age relationships are uncertain. The mafic intrusive rocks likely include both synvolcanic and younger successor-arc intrusions. They have been grouped as one map unit solely on the basis of their similar compositions.

### Gabbro, diorite to quartz diorite (unit 8a)

Medium- to fine-grained gabbro and diorite (dolerite) dikes intrude massive mafic flows and rhyolite in the north-central and northeastern parts of the map area. These are interpreted to be high-level synvolcanic intrusions, part of the gabbro–diorite–quartz diorite–tonalite series that is prevalent in the Flin Flon arc assemblage (Syme et al., 1998).

Gabbro weathers medium green to buff and is dark green on fresh surfaces. Fine-grained dikes are difficult to distinguish from enclosing massive mafic flows. They often take the form of irregularly shaped dikes and patchy zones.

The gabbro is composed of 35–45% subhedral plagioclase, 40% pyroxene (primarily altered to a combination of chlorite, tremolite-actinolite and minor biotite) and accessory minerals that include 3–5% interstitial quartz, 2–3% pyrite-pyrrhotite and variable (1–5%) carbonate. Gabbro dikes in the north-central part of the area commonly contain trace to 2% magnetite as subhedral crystals. Grain size is variable, ranging from 1 to 3 mm for medium-grained varieties to <1 to 1 mm for fine-grained doleritic types. Gabbro textures are commonly hypidiomorphic to ophitic.

Diorite is composed of 35–40% plagioclase, 25–40% hornblende (variably altered to chlorite and tremolite-actinolite), 5–10% alkali feldspar and 0–5% biotite. Diorite commonly contains 5–7% quartz. Thin section analysis shows that plagioclase is commonly pervasively altered to sericite and locally contains myrmekitic quartz intergrowths. Free quartz is interstitial to feldspar and hornblende. The unit typically has an ophitic texture.

#### Diabase (unit 8b)

Medium- to coarse-grained diabase dikes intrude and crosscut volcanic supracrustal rocks at an acute angle to stratigraphy in the central part of the map area. Where exposed, the dikes vary in thickness from a few metres up to 200 m, the latter being the width of the large dike in the central part of the map area. The diabase has a brown-green weathered colour and is mottled beige and dark green on fresh surfaces. Macroscopically, the unit has an ophitic texture and is composed of 35% hornblende (after pyroxene) ±chlorite, 60% plagioclase and 2–5% pyrite±pyrrhotite±magnetite. In thin section, the plagioclase was observed to be pervasively altered to sericite. Diabase dikes are interpreted to be the second youngest unit in the area because they intrude all volcanic sequences. Xenoliths of diabase are enclosed within the quartz porphyritic granite (unit 9a) in the central and eastern parts of the map area. The age relationship with the granodiorite intrusion east of Persian Lake is uncertain.

#### Feldspar porphyry (unit 8c)

A distinctive feldspar porphyry of intermediate composition intrudes mafic and felsic volcanic rocks on the southwest side of Persian Lake. This unit weathers dark green-grey and contains approximately 10% beige to greenish, 1–3 mm, subhedral plagioclase phenocrysts set in a medium-grained, weakly foliated matrix composed of hornblende, chlorite and plagioclase.

### *Felsic intrusions (unit 9)*

#### Quartz (±feldspar) porphyritic granite-granodiorite (unit 9a)

This unit, interpreted to be the youngest in the area, intrudes mafic and felsic flows and diabase in the central and northeastern parts of the map area. It is orange-beige on weathered surfaces and composed of 1–20% angular to subrounded quartz phenocrysts, 1–7 mm in size, in a medium-grained groundmass of 40–50% quartz, 20% potassium feldspar, 15% plagioclase and 15–20% hornblende. Content of alkali feldspar phenocrysts (when present) varies from 1 to 15% and occur as 1–6 mm, subhedral, cream to pinkish crystals. Microscopically, feldspars are strongly altered and contain abundant sericite and carbonate. Hornblende is commonly altered to a combination of chlorite and actinolite, with minor amounts of epidote and biotite present.

The wedge-shaped body in the central part of the map area contains metre-size angular to subrounded xenoliths of diabase on its eastern margin and xenoliths of mafic volcanic rocks near its fault-bounded northern boundary The fault that truncates this intrusive body on its northern margin is over 20 km in length and extends from the North Arm of Athapapuskow Lake east and northeast to Nesosap Lake (Syme et al., 1998). A faulted extension of this unit is exposed as a thin linear mass west of Pothook Lake.

#### Granodiorite (unit 9b)

This unit is exposed on the eastern shore of Persian Lake and dominates the area east of this map area. It is medium to coarse grained and has a buff-pink weathered surface and mottled orange and black fresh surface. Compositionally, the unit consists of 40% potassium feldspar, 30% quartz, 5% plagioclase, 15% hornblende and 10% biotite. The unit is massive except close to Persian Lake, where it contains a moderate to strong shear fabric with a north-northeast orientation. Granite pegmatite veins fill fractures in the granodiorite close to the Persian Lake shoreline.

## Geochemistry

Systematic detailed mapping of the Flin Flon Belt (Bailes and Syme, 1989), geochemical studies (Stern et al., 1995; Syme, 1998) and tectonic synthesis (Lucas et al., 1996) show the Flin Flon Belt to comprise volcanosedimentary assemblages derived from a variety of tectonic environments. During mapping of the Thompson Bay–Persian Lake area, 17 samples were collected and submitted for geochemical analysis (Tables 1 and 2). Eleven of the samples were mafic and six were felsic in composition. Ten of the samples (seven mafic and three felsic) were submitted to the University of Saskatchewan for inductively coupled plasma–mass spectrometry (ICP-MS). Geochemistry of these samples has been used to determine their geochemical affinity (Figures 7 and 8).

Volcanic rocks from the Thompson Bay–Persian Lake area are subalkaline and range from basalt to rhyolite in composition (Figure 7a). The mafic volcanic rocks gradually increase in

**Table 1: Major-element composition of rock samples from the Thompson Bay–Persian Lake area.**

| Sample | Rock type | $SiO_2$ (%) | $Al_2O_3$ (%) | $Fe_2O_3$ (%) | MnO (%) | MgO (%) | CaO (%) | $Na_2O$ (%) | $K_2O$ (%) | $TiO_2$ (%) | $P_2O_5$ (%) | LOI | Total |
|---|---|---|---|---|---|---|---|---|---|---|---|---|---|
| 300 | Basaltic andesite, feldspar phyric | 59.22 | 14.91 | 11.65 | 0.19 | 3.5 | 4.02 | 2.63 | 1.89 | 0.43 | 0.25 | 1.33 | 100.03 |
| 301 | Basalt, aphyric | 51.03 | 17.83 | 13.36 | 0.21 | 3.66 | 6.12 | 3.44 | 2.48 | 0.62 | 0.39 | 0.84 | 99.97 |
| 302 | Basalt, aphyric | 57.79 | 14.59 | 11.15 | 0.17 | 3.61 | 7.27 | 2.79 | 0.74 | 0.62 | 0.12 | 0.87 | 99.71 |
| 303 | Basalt, pillowed flow, vesicular | 55.47 | 13.59 | 17.09 | 0.18 | 4.92 | 0.97 | 1.99 | 0.51 | 0.68 | 0.3 | 4 | 99.69 |
| 304 | Rhyolite, massive, aphyric | 72.64 | 12.33 | 4.43 | 0.07 | 4.19 | 0.15 | 1.5 | 2.26 | 0.23 | 0.08 | 2.75 | 100.61 |
| 305 | Basalt, pillowed flow, feldspar phyric, vesicular | 48.96 | 14.66 | 9.45 | 0.14 | 6.51 | 6.78 | 3.61 | 1.02 | 0.45 | 0.09 | 7.79 | 99.46 |
| 306 | Rhyolite, massive, aphyric | 74.76 | 11.47 | 4.56 | 0.02 | 1.79 | 0.54 | 3.94 | 1 | 0.27 | 0.07 | 1.86 | 100.28 |
| 308 | Basalt, pillowed flow, feldspar phyric | 50.69 | 15.76 | 9.21 | 0.15 | 6.98 | 9.52 | 3.99 | 0.28 | 0.33 | 0.04 | 2.41 | 99.38 |
| 310 | Andesite/dacite(?) | 56.41 | 14.36 | 13.32 | 0.19 | 4.38 | 7.13 | 2.84 | 0.45 | 0.67 | 0.09 | 0.41 | 100.24 |
| 314 | Andesite/dacite(?) dike | 58.57 | 14.97 | 9.66 | 0.12 | 6.08 | 4.46 | 4.86 | 0.42 | 0.47 | 0.08 | 0.5 | 100.19 |
| 315 | Rhyolite, massive, 1% quartz phyric | 73.49 | 11.61 | 5.06 | 0.06 | 2.26 | 3.6 | 0.93 | 1.48 | 0.27 | 0.08 | 1.89 | 100.73 |
| 319 | Rhyolite, massive, aphyric | 68.22 | 12.69 | 7.67 | 0.1 | 1.99 | 2.36 | 4.78 | 0.27 | 0.42 | 0.1 | 0.81 | 99.41 |
| 320 | Dacite(?) | 64.29 | 13.54 | 9.3 | 0.12 | 2.83 | 2.17 | 4.4 | 1.67 | 0.62 | 0.12 | 0.58 | 99.63 |
| 326 | Basaltic andesite, feldspar-pyroxene phyric | 57.42 | 12.61 | 8.05 | 0.06 | 5.3 | 3.36 | 4.28 | 1.28 | 0.51 | 0.1 | 6.85 | 99.81 |
| 327 | Basalt, massive | 55.92 | 14.1 | 11.71 | 0.1 | 5.27 | 1.58 | 4.21 | 1.43 | 0.7 | 0.3 | 4.38 | 99.7 |
| 328 | Basaltic andesite, massive, aphyric | 57.59 | 13.61 | 14.42 | 0.15 | 5.1 | 0.48 | 0.98 | 1.48 | 0.74 | 0.14 | 4.32 | 99.01 |
| 329 | Rhyolite, lobe, aphyric | 78.55 | 9.95 | 4.57 | 0.08 | 0.87 | 0.58 | 4.21 | 0.44 | 0.29 | 0.15 | 0.96 | 100.64 |

| Sample | Rock type | Ba (ppm) | Sr (ppm) | Y (ppm) | Sc (ppm) | Zr (ppm) | Be (ppm) | V (ppm) |
|---|---|---|---|---|---|---|---|---|
| 300 | Basaltic andesite, feldspar phyric | 668 | 169 | 15 | 30 | 57 | 2 | 114 |
| 301 | Basalt, aphyric | 753 | 347 | 19 | 40 | 65 | 2 | 174 |
| 302 | Basalt, aphyric | 445 | 241 | 15 | 36 | 58 | 1 | 270 |
| 303 | Basalt, pillowed flow, vesicular | 71 | 23 | 10 | 32 | 43 | -1 | 86 |
| 304 | Rhyolite, massive, aphyric | 52 | 32 | 17 | 14 | 87 | -1 | 31 |
| 305 | Basalt, pillowed flow, feldspar phyric, vesicular | 150 | 103 | 6 | 40 | 24 | -1 | 213 |
| 306 | Rhyolite, massive, aphyric | 312 | 49 | 24 | 13 | 113 | -1 | -5 |
| 308 | Basalt, pillowed flow, feldspar phyric | 146 | 88 | 3 | 49 | 12 | 1 | 284 |
| 310 | Andesite/dacite(?) | 211 | 173 | 10 | 43 | 39 | 2 | 339 |
| 314 | Andesite/dacite(?) dike | 363 | 129 | 11 | 39 | 45 | 1 | 226 |
| 315 | Rhyolite, massive, 1% quartz phyric | 339 | 47 | 16 | 17 | 82 | -1 | 32 |
| 319 | Rhyolite, massive, aphyric | 70 | 70 | 17 | 21 | 74 | -1 | 45 |
| 320 | Dacite(?) | 323 | 122 | 15 | 30 | 67 | -1 | 38 |
| 326 | Basaltic andesite, feldspar-pyroxene phyric | 228 | 47 | 14 | 28 | 46 | -1 | 208 |
| 327 | Basalt, massive | 402 | 79 | 14 | 33 | 43 | -1 | 114 |
| 328 | Basaltic andesite, massive, aphyric | 305 | 12 | 11 | 33 | 53 | 2 | 326 |
| 329 | Rhyolite, lobe, aphyric | 207 | 54 | 17 | 15 | 58 | -1 | -5 |

**Table 2: Trace-element composition of rock samples from the Thompson Bay–Persian Lake area. All values in ppm.**

| Sample | Rock type | Li | P | Sc | Ti | V | Cr | Co | Ni | Cu | Zn | Rb | Sr | Y | Zr | Nb | Mo | Cd | Sn | Sb | Cs | Ba | La |
|---|---|---|---|---|---|---|---|---|---|---|---|---|---|---|---|---|---|---|---|---|---|---|---|
| 329-1 | Rhyolite, lobe, aphyric | 5.63 | 553 | 15.68 | 1805 | 3.97 | 2 | 28.42 | 1.07 | 30.55 | 72.05 | 4.73 | 57.49 | 16.62 | 67.23 | 4.9 | 0.91 | 0.06 | 0.76 | 0.28 | 0.54 | 217.41 | 11.35 |
| 314-1 | Andesite/dacite(?), dyke | 2.64 | 299 | 40.15 | 2864 | 262.16 | 15 | 41.59 | 15.51 | 2.32 | 21.96 | 5.73 | 141.02 | 11.99 | 49.48 | 3.34 | 0.55 | 0.05 | 0.49 | 0.10 | 0.44 | 371.49 | 7.17 |
| 305-1 | Basalt, pillowed flow | 14.34 | 300 | 44.74 | 2770 | 278.04 | 79 | 41.29 | 25.97 | 91.96 | 75.81 | 5.62 | 112.22 | 7.49 | 23.17 | 1.55 | 0.19 | 0.08 | 0.28 | 0.30 | 0.46 | 155.28 | 2.85 |
| 302-1 | Basalt, massive, aphyric | 10.43 | 411 | 37.99 | 3798 | 312.25 | 19 | 50.75 | 26.69 | 116.22 | 77.30 | 9.72 | 259.26 | 14.93 | 55.71 | 4.48 | 1.27 | 0.16 | 0.64 | 0.26 | 0.52 | 467.7 | 7.71 |
| 327-1 | Basalt, massive | 16.44 | 1199 | 34.79 | 4332 | 158.32 | 5 | 37.48 | 5.71 | 97.77 | 87.82 | 11.56 | 88.31 | 13.64 | 45.61 | 3.27 | 0.35 | 0.08 | 0.38 | 0.47 | 0.44 | 409.99 | 8.58 |
| 320-1 | Dacite(?) | 10.23 | 474 | 31.14 | 4100 | 73.03 | 2 | 42.72 | 1.15 | 9.92 | 53.87 | 21.71 | 130.58 | 15.35 | 72.82 | 5.18 | 0.92 | 0.04 | 1.19 | 0.09 | 0.68 | 329.76 | 10.74 |
| 301-1 | Basalt, massive, aphyric | 14.2 | 1553 | 38.44 | 3868 | 214.03 | 1 | 43.71 | 5.14 | 27.09 | 132.95 | 43.07 | 351.36 | 18.57 | 67.03 | 4.18 | 0.57 | 0.12 | 0.77 | 0.10 | 0.78 | 769.32 | 12.42 |
| 319-1 | Rhyolite, massive, aphyric | 0.54 | 459 | 24.6 | 2648 | 77.35 | 1 | 40.12 | 3.16 | 5.07 | 46.95 | 2.06 | 78.17 | 16.98 | 86.34 | 6.19 | 1.04 | 0.04 | 0.81 | 0.14 | 0.32 | 72.61 | 11.75 |
| 308-1 | Basalt, pillowed flow, feldspar phyric | 6 | 118 | 50.23 | 2022 | 320.89 | 279 | 51.35 | 60.45 | 85.38 | 54.86 | 2.18 | 90.83 | 3.78 | 10.43 | 0.83 | 0.51 | 0.04 | 0.28 | 0.19 | 0.37 | 147.6 | 2.3 |
| 300-1 | Basaltic andesite, 5–7% feldspar phyric | 9.93 | 902 | 28.99 | 2595 | 156.26 | 4 | 33.13 | 3.51 | 68.06 | 84.15 | 38.44 | 171.82 | 15.45 | 60.55 | 4.23 | 0.98 | 0.10 | 1.26 | 0.21 | 0.64 | 707.05 | 11.85 |

| Sample | Rock type | Ce | Pr | Nd | Sm | Eu | Gd | Tb | Dy | Ho | Er | Tm | Yb | Lu | Hf | Ta | W | Tl | Pb | Bi | Th | U |
|---|---|---|---|---|---|---|---|---|---|---|---|---|---|---|---|---|---|---|---|---|---|---|
| 329-1 | Rhyolite, lobe, aphyric | 23.86 | 2.95 | 12.35 | 3.02 | 0.66 | 2.91 | 0.43 | 2.83 | 0.62 | 1.76 | 0.27 | 1.73 | 0.28 | 1.83 | 0.87 | 143.62 | 0.03 | 2.03 | 0.05 | 2.24 | 0.73 |
| 314-1 | Andesite/dacite(?), dyke | 15.05 | 1.92 | 8 | 1.89 | 0.55 | 1.97 | 0.29 | 1.98 | 0.43 | 1.27 | 0.19 | 1.31 | 0.2 | 1.35 | 0.61 | 111.32 | 0.02 | 0.7 | 0.19 | 2.84 | 0.54 |
| 305-1 | Basalt, pillowed flow | 6.61 | 0.88 | 3.89 | 1.06 | 0.37 | 1.17 | 0.18 | 1.33 | 0.3 | 0.84 | 0.12 | 0.87 | 0.14 | 0.69 | 0.14 | 21.70 | 0.01 | 1.21 | 0.08 | 1.96 | 0.21 |
| 302-1 | Basalt, massive, aphyric | 17.19 | 2.2 | 9.2 | 2.25 | 0.66 | 2.39 | 0.37 | 2.55 | 0.56 | 1.61 | 0.24 | 1.6 | 0.24 | 1.66 | 0.78 | 161.58 | 0.07 | 2.47 | 0.18 | 2 | 0.64 |
| 327-1 | Basalt, massive | 18.66 | 2.41 | 10.6 | 2.45 | 0.8 | 2.65 | 0.39 | 2.53 | 0.55 | 1.58 | 0.22 | 1.44 | 0.24 | 1.2 | 0.3 | 38.51 | 0.09 | 1.66 | 0.14 | 1.41 | 0.42 |
| 320-1 | Dacite(?) | 22.5 | 2.69 | 10.92 | 2.46 | 0.79 | 2.72 | 0.39 | 2.78 | 0.6 | 1.84 | 0.28 | 1.96 | 0.31 | 2.09 | 0.8 | 166.35 | 0.1 | 2.12 | 0.04 | 2.98 | 0.94 |
| 301-1 | Basalt, massive, aphyric | 27.67 | 3.59 | 15.26 | 3.65 | 1.11 | 3.8 | 0.53 | 3.48 | 0.71 | 2.06 | 0.32 | 2.16 | 0.33 | 2.03 | 0.46 | 84.35 | 0.22 | 4.55 | 0.16 | 2.1 | 1.17 |
| 319-1 | Rhyolite, massive, aphyric | 24.84 | 3.04 | 12.07 | 2.76 | 0.76 | 2.9 | 0.45 | 3.11 | 0.66 | 1.93 | 0.29 | 1.92 | 0.31 | 2.48 | 1.17 | 235.38 | 0 | 2.91 | 0.15 | 3.16 | 0.95 |
| 308-1 | Basalt, pillowed flow, feldspar phyric | 4.77 | 0.62 | 2.71 | 0.64 | 0.26 | 0.69 | 0.11 | 0.73 | 0.16 | 0.47 | 0.07 | 0.45 | 0.07 | 0.38 | 0.28 | 69.42 | 0.02 | 1.97 | 0.09 | 1.35 | 0.16 |
| 300-1 | Basaltic andesite, 5–7% feldspar phyric | 25.09 | 3.26 | 13.64 | 3.06 | 0.84 | 3.09 | 0.43 | 2.77 | 0.56 | 1.67 | 0.25 | 1.6 | 0.27 | 1.63 | 0.56 | 101.21 | 0.18 | 1.54 | 0.18 | 1.87 | 1.08 |

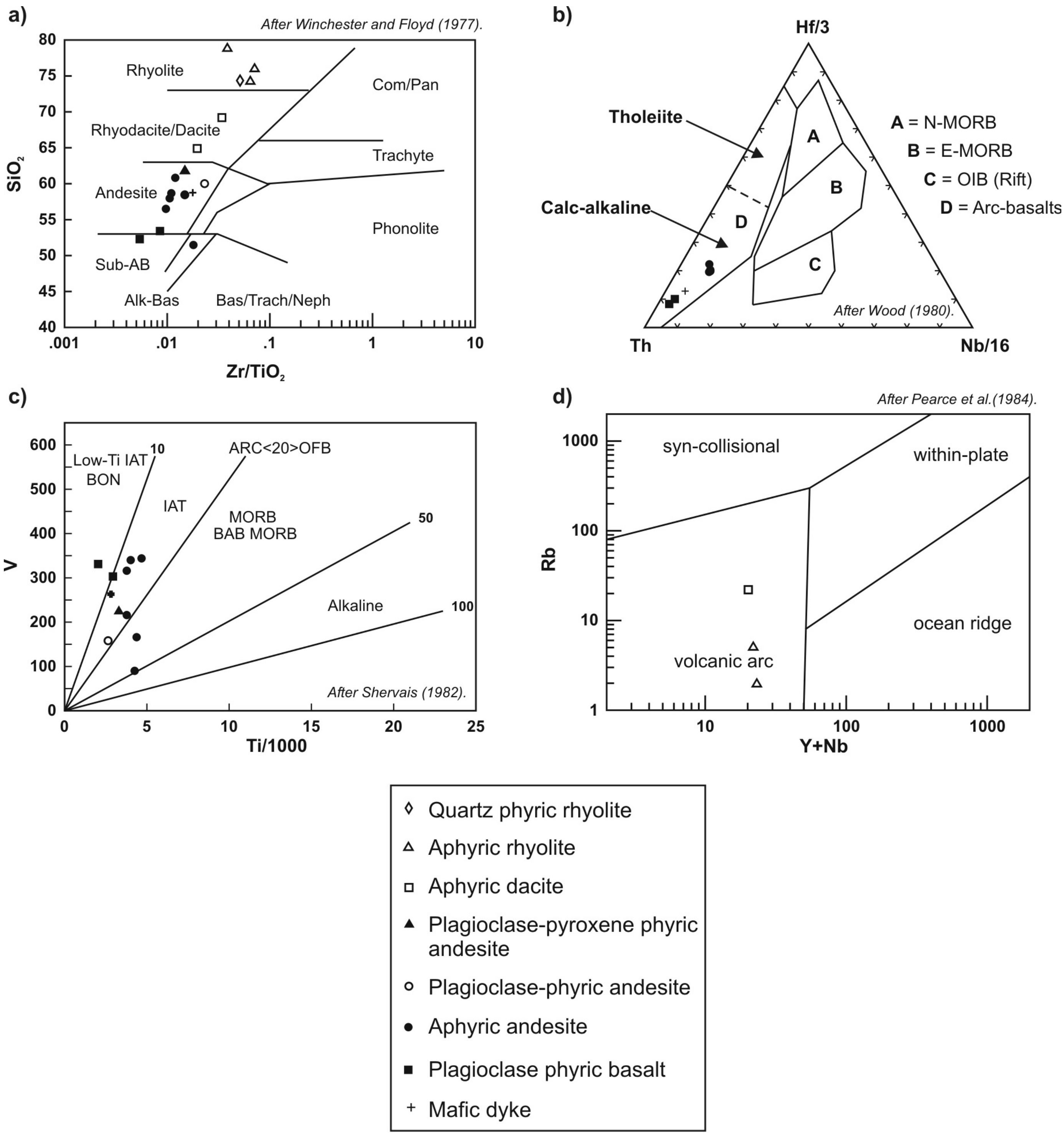


***Figure 7:*** *Rock samples from the Thompson Bay–Persian Lake area plotted on various volcanic discrimination diagrams: a) $SiO_2$ vs. $Zr/TiO_2$ (*after *Winchester and Floyd, 1977), b) Th vs. Hf/3 vs. Nb/16 (*after *Wood 1980), c) V vs. Ti/100 (*after *Shervais, 1982), and d) Rb vs. Y+Nb (*after *Pearce et al., 1984). Abbreviations: Alk-Bas, alkaline basalt; BAB, back arc basin; Bas/Trach/Neph, basalt/trachybasalt/nephelinite; Bon, boninite; Com/Pac, comendite/pantellerite; IAT, island arc tholeiite; OFB, ocean floor basalt; Sub-AB, subalkaline basalt.*

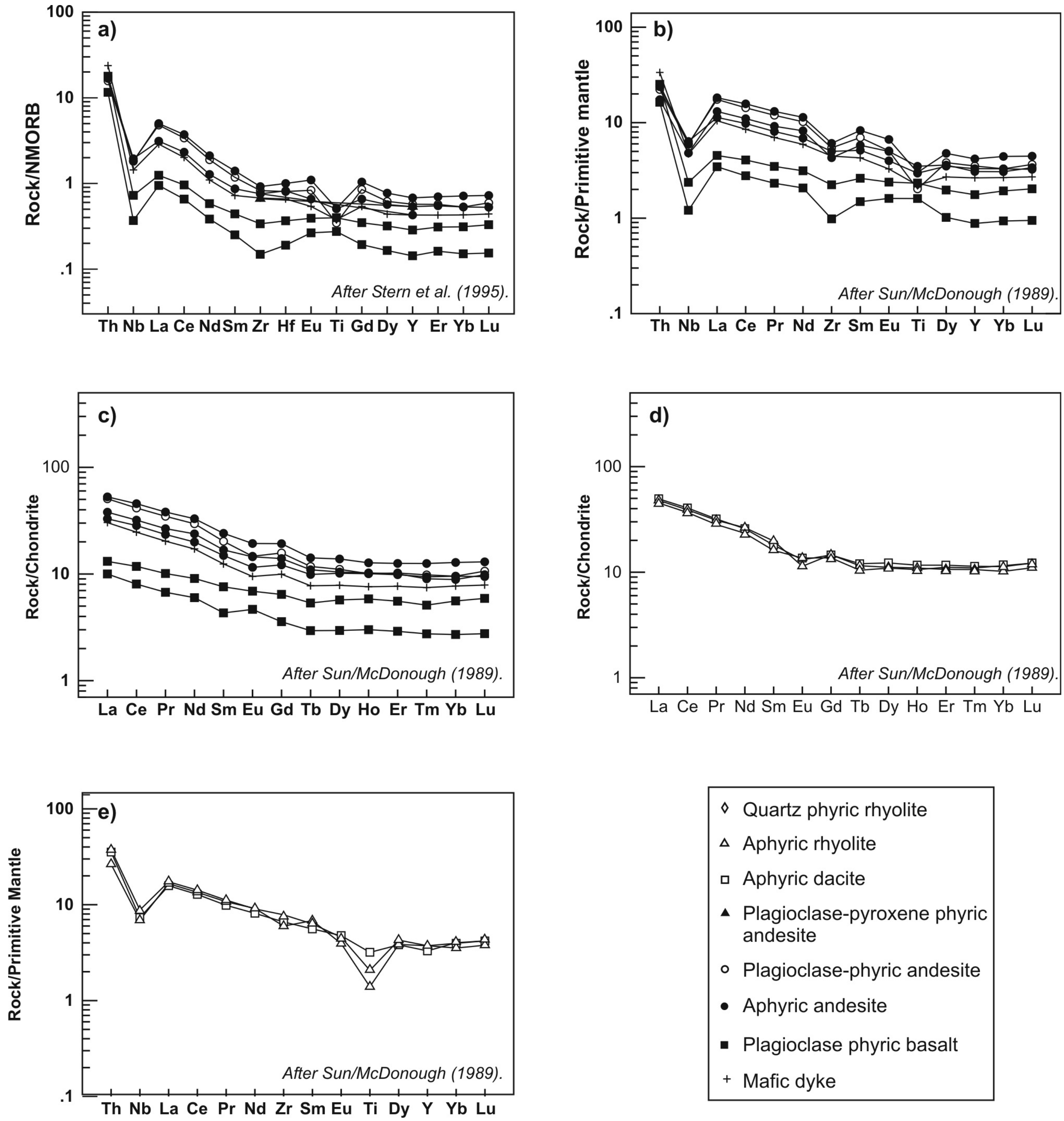


***Figure 8:*** *Rock samples from the Thompson Bay–Persian Lake area plotted on extended trace element diagrams: a) mafic rocks normalized against normal mid-ocean ridge basalt (N-MORB;* after *Stern et al., 1995), b) mafic rocks normalized against primitive mantle (*after *Sun and McDonough, 1989), c) rare earth element contents of mafic rocks normalized against chondrite (*after *Sun and McDonough, 1989), d) rare earth element contents of felsic rocks normalized against chondrite (*after *Sun and McDonough, 1989), and e) felsic rocks normalized against primitive mantle (*after *Sun and McDonough, 1989).*

silica content upward through the stratigraphic section (toward the southwest). Trace-element geochemistry of mafic (Figure 7b and 7c) and felsic (Figure 7d) samples indicate that they were erupted in an oceanic island arc tectonic regime. The high Th to Hf/3 ratio (Figure 7b) of mafic volcanic rocks indicates a calcalkaline geochemical affinity for the sequence.

Extended trace element plots (using only immobile elements) of mafic volcanic rocks, normalized to normal mid-ocean ridge basalt (N-MORB; Figure 8a) and primitive mantle (Figure 8b), display the diagnostic negative Nb and elevated Th values of subduction-generated volcanic-arc basalt (Pearce, 1996). They also display the slight depletion of Zr and Ti, relative to N-MORB and primitive mantle, that is typical of subduction-generated magmas. The mafic volcanic rocks display two separate geochemical signatures. Two samples (both plagioclase-phyric basalt) have low rare earth element (REE) content (Figure 8c) and higher MgO content (>6.5%, Table 1). The remaining samples are andesite with higher overall REE content (Figure 8c) and lower MgO (3.5–6%, Table 1). Both groups display elevated light rare earth element (LREE) contents (Figure 8c) and depletion in Zr (Figure 8a and 8b). The two basalt samples do not display Ti depletion, but the andesite does show Ti depletion relative to N-MORB and primitive mantle (Figures 8a and 8b).

Trace and rare earth element geochemistry of felsic volcanic rocks in the Thompson Bay–Persian Lake area indicates that they are geochemically most similar to the andesite. They display identical REE content (compare Figure 8c and 8d) and Ti depletion (compare Figure 8b and 8e), as do the andesite. Their trace and rare earth element geochemistry is consistent with a calcalkaline affinity. Specifically, the Thompson Bay–Persian Lake rhyolite exhibits

1) LREE enrichment,
2) small negative Eu anomaly (Eu/Eu* = 0.7 – 0.8),
3) flat HREE patterns,
4) moderate $La/Yb_n$ ratios of approximately 4–5, and
5) Zr/Y ratios of 4–5.

These characteristics and other trace element abundances correspond to those of calcalkaline rhyolite in the central Flin Flon Belt (Syme, 1998). Trace element abundances and ratios also correspond to those shown by FII and FIIIa type rhyolites of Lesher et al. (1986), except that they have lower Zr and Hf contents; however, these two elements are known to have lower abundances in other rhyolite in the central Flin Flon Belt (Gale and Dabek, 1996; Syme, 1998).

## Structural geology

Volcanic rocks in the western part of the map area include northeast- to east-trending flows that are overprinted by a bedding-parallel north-northeast-trending schistosity. Mineralized north-trending shears and faults associated with the North Arm Fault are abundant along the east shore of Thompson Bay. The north shore area of Sharpe Bay is also extensively sheared. Shears in the central Sharpe Bay area have a north-northeast orientation, which changes to an east-northeast direction at the east end of the bay.

Mafic pillowed flows are reasonably well preserved only in the western part of the map area. Facing directions indicated by pillow tops suggest the area is primarily a monoclinal, southeast-facing sequence. The only exception is in the northwest corner near the Hotstone occurrence, where pillowed flows indicate a north-northwest facing direction. This suggests the presence of an anticlinal structure in this area. Foliations in the area indicate that the anticline is overturned to the northwest.

Numerous known and presumed faults that offset units to various extents are present throughout the map area. Large-scale east-trending faults occur in the northern, southern and central parts of the area. Smaller scale faults with a north to northeasterly orientation occur in the western and central parts of the map area.

Volcanic sequences at Persian Lake have a northerly trend that changes to northeasterly west of the lake. Schistosities, which are typically poorly preserved, are overprinted by a prevalent north-northeast-trending (020º) foliation. Volcanic rocks are generally fine grained and massive. Felsic volcanic rocks occasionally display a faint biotite foliation. Late east- and northeast-trending sinistral faults with a small strike-slip component cut sequences at and west of Persian Lake. The area west of Persian Lake is structurally complex, and lack of primary structures (e.g., facing indicators, marker horizons, etc.) makes interpretation difficult.

Outcrop patterns approximately 700 m west of Persian Lake, observed from airphotos, suggest the presence of a fold hinge with a northeast-trending axial plane. This structure is not obvious in the field. The repetitive layered nature of units within this area suggests the possibility of a sequence of tightly folded isoclinal folds. Outcrop surfaces in the Persian Lake area (especially west of the lake) are highly fractured. Fractures have a somewhat random orientation; however, a couple of the more prominent orientations are southeast (210°–230°) and east (80°–110°). The fractures are relatively flat lying (40°–50°) to moderately dipping (60°–70°). Quartz veins and silica veinlets frequently fill fractures with similar orientations.

The dominant north-northeast foliation throughout the map area is believed to represent $S_1$. The only other planar fabric observed throughout the map area is associated with shear and fault zones. As previously mentioned, north-trending shears and faults overprint the schistosity in the Thompson Bay area. In the central and Persian Lake areas, northeast-trending shears and faults overprint $S_1$ and sometimes impart a weak crenulation cleavage.

## Economic geology

Several documented mineral occurrences exist within the project area (Gale and Eccles, 1992), with the majority of them concentrated in the central part of the area. These occurrences consist primarily of stratabound massive sulphide deposits with minor chalcopyrite and some form of associated alteration zone. The majority of the occurrences are hosted within felsic to intermediate volcanic rocks that are commonly sheared and/or silicified. Nearly all of them have been tested by shallow to intermediate (75–150 m vertical depth) drillholes and trenching. Most have been adequately tested and geophysical conductors have been explained. Nevertheless, given the structural complexity, lack of facing indicators (in the eastern part of the map area) and the abundance of alteration, it is unlikely that all alteration zones have been tested to their stratigraphic tops.

Potential also exists with zones of alteration that have no record of being tested. An extensively chloritized massive rhyolite unit, situated just west of the large diabase dike in the south-central part of the map area, is a good example. At this location, green-black anastomosing chloritic stringers and irregularly shaped clots up to 10 cm in diameter impart a net texture to the rhyolite unit (Figure 9). This type of alteration is typically found in the footwall of proximal volcanogenic massive sulphide deposits (e.g., Flin Flon, Schist Lake, Mandy and Centennial; Bailes and Syme, 1989). Sheared and altered coarse fragmental rhyolite lies 60–80 m west of the strongly chlorite-altered exposure. Other zones of chlorite alteration and a garnet-anthophyllite alteration zone with associated sulphide mineralization warrant additional investigation. An iron-magnesium alteration zone, measuring approximately 20 m by 5 m, occurs in an in situ rhyolite breccia 600 m southwest and along strike from the Hotstone occurrence. The alteration zone contains angular to subangular rhyolite fragments in a chlorite-rich matrix with a patchy quartz vein network. Chlorite alteration veins and quartz veins also occur within massive basaltic andesite just east of the Hotstone occurrence.

A large gossan zone (~130 m by 25 m) partially subcrops 600 m west of the junction of the hydro line and the logging road in the eastern part of the map area. The gossan is hosted by sheared and silicified basaltic andesite. Sulphide mineralization consists of 2–4%, and locally up to 10%, pyrite.

As noted, there are many known and presumed faults and shear zones throughout the map area. Many of these have associated quartz veins and silicification. Most of the exposed quartz veins observed are narrow (<0.5 m), barren or contain minor pyrite or pyrrhotite. There are, however, large areas of swamp and overburden cover that overlie presumed fault zones, and it is unlikely that these have been tested by induced polarization surveys.

Oxide-facies iron formations (locally massive sulphide) in the central part of the map area and west of Persian Lake are potential hosts for gold mineralization. The iron formations observed, however, are relatively narrow and have moderate to low sulphide content. Sulphide-bearing chert layers up to 15 m thick are exposed in the central part of the map area. An approximately 0.5 m thick chert layer, exposed in an overgrown trench, contains 3–4% fine-grained arsenopyrite needles and blebs with 1–2 mm chlorite veinlets. There is no known documentation of this occurrence.

West of Pothook Lake in the northeastern part of the map area, an occurrence of stringers and blebs of pyrite, pyrrhotite, chalcopyrite and sphalerite occurs within a quartz porphyry intrusion (Gale and Eccles, 1992). The quartz porphyry intrudes mafic and felsic volcanic and gabbroic rocks. One of the samples assayed from this occurrence contained 6.0 g/t gold. A larger faulted mass of this intrusion occurs in the central part of the map area.

Prospecting work by B. Murray in 2001 located a new high-grade copper occurrence very close to the hydro line in the north-central part of the map area. Subsequent mapping was conducted by M'Ore Exploration. Bell Resources optioned the property and carried out trenching, mapping and geophysics in 2002. The occurrence consists of massive to semimassive sulphides, primarily chalcopyrite and pyrite, within a brecciated rhyolite unit. Assay values of 4% copper, trace zinc and up to 0.75 g/t gold were reported from surface grab samples (Bell Resources Corporation, unpublished company information, 2003). Bell claimed that the discovery is associated with a significant VLF-EM anomaly and a showing of copper-gold mineralization 200 m to the west, where values of 4% copper and 1.37–6.17 g/t gold were found in trench samples. Bell conducted a drill program on the new showing in early 2003, but assay results were not made available.

***Figure 9:*** *Massive aphyric rhyolite mottled with patches of chlorite, south-central part of map area.*

## Acknowledgments

George Gale mapped the northeastern corner of the map area and assisted with geological interpretation and project planning. Student assistants Chris Kelly and Adrienne Hanly provided capable assistance during field mapping. Rock sample processing and crushing were carried out by the Manitoba Geological Survey Laboratory under the supervision of Doug Berk; geochemical analyses were undertaken at the University of Saskatchewan (Saskatoon) and at Activation Laboratories Ltd. (Ancaster, Ontario). Bonnie Lenton produced the digital figures and Maureen McFarlane digitized the geology map. Alan Bailes and Paul Gilbert assisted with the geochemistry interpretation. Editorial assistance was provided by Alan Bailes, Tim Corkery and Bob Davie of RnD Technical (Peterborough, Ontario). The author extends sincere gratitude to all individuals who assisted in the field mapping, rock sample processing and report production processes.

## References

Bailes, A.H. and Syme, E.C. 1989: Geology of the Flin Flon–White Lake area; Manitoba Energy and Mines, Minerals Division, Geological Report GR 87-1, 313 p.

Buckham, A.F. 1944: Athapapuskow Lake, Manitoba (NTS 63K/12); Geological Survey of Canada, Map 807A, scale 1:63 360.

Dolozi, M.B. and Ayres, L.D. 1991: Early Proterozoic basaltic andesite tuff breccia: downslope, subaqueous mass transport of phreatomagmatically-generated tephra; Bulletin of Volcanology, v. 53, p. 477–495.

Gale, G.H. and Dabek, L.B. 1996: The Baker Patton Complex (parts of 63K/12 and 63K/13) — rhyolites, dacites and rare earth element chemistry; *in* Report of Activities 1996, Manitoba Energy and Mines, Geological Services, p. 47–51.

Gale, G.H. and Dabek, L.B. 2002: Geology of the Baker Patton Complex, Flin Flon, Manitoba (parts of NTS 63K 12, 13); Manitoba Industry, Trade and Mines, Manitoba Geological Survey, Geoscientific Map MAP2002-1, scale 1:10 000.

Gale, G.H. and Eccles, D.R. 1992: Mineral deposits and occurrences in the Schist Lake area, NTS 63K/12; Manitoba Energy and Mines, Mineral Deposit Series Report 11, 233 p.

Gale, G.H., Dabek, L.B., Prouse, D.E. and Norquay, L.I. 1994: Baker Patton Felsic Complex (parts of 3K/13 and 63K/12); *in* Report of Activities 1994, Manitoba Energy and Mines, Geological Services, p. 61–63.

Hoffman, P.F. 1988: United plates of America, the birth of a craton: Early Proterozoic assembly and growth of Laurentia; Annual Reviews of Earth and Planetary Science, v.16, p. 543–603.

Lesher, C.M., Goodwin, A.M., Campbell, I.H. and Gorton, M.P. 1986: Trace-element geochemistry of ore-associated and barren, felsic metavolcanic rocks in the Superior Province Canada; Canadian Journal of Earth Sciences, v. 23, p. 222–237.

Lucas, S.B., Stern, R.A., Syme, E.C., Reilly. B.A. and Thomas, D.J. 1996: Intraoceanic tectonics and the development of continental crust: 1.92–1.84 Ga evolution of the Flin Flon Belt, Canada; Geological Society of America Bulletin, v. 108, p. 602–629.

Pearce, J.A. 1996: A user's guide to basalt discrimination diagrams; *in* Trace Element Geochemistry of Volcanic Rocks: Applications for Massive Sulphide Exploration, D.A. Wyman (ed.), Geological Association of Canada, Short Course Notes, v. 12, p. 79–113.

Pearce, J.A., Harris, N.B.W. and Tindle, A.G. 1984: Trace element discrimination diagrams for tectonic interpretation of granitic rocks; Contributions to Mineralogy and Petrology, v.25, p. 956–983.

Prouse, D.E. 1995: The Hotstone-Cleaver Lake project, North Arm, Lake Athapapuskow, (NTS 63K/12); *in* Report of Activities 1995, Manitoba Energy and Mines, Geological Services, p. 34–37.

Prouse, D.E. 1996: The Hotstone-Persian Lake project; North Arm, Lake Athapapuskow (NTS 63K/12); *in* Report of Activities 1996, Manitoba Energy and Mines, Geological Services, p. 43–46.

Shervais, J.W. 1982: Ti-V plots and the petrogenesis of modern and ophiolitic lavas; Earth and Planetary Science Letters, v. 59, p. 101–118.

Stern, R.A., Syme, E.C., Bailes, A.H. and Lucas, S.B. 1995: Paleoproterozoic (1.90–1.86 Ga) arc volcanism in the Flin Flon Belt, Trans-Hudson Orogen, Canada; Contributions to Mineralogy and Petrology, v. 119, p. 117–141.

Sun, S.S. and McDonough, W.F. 1989: Chemical and isotopic systematics of oceanic basalts: implications for mantle composition and processes; *in* Magmatism in the Ocean Basins, A.D. Saunders and M.J. Norry (ed.), Geological Society of London, Special Publication 42, p. 313–345.

Syme, E.C. 1998: Ore-associated and barren rhyolites in the central Flin Flon belt: case study of the Flin Flon mine sequence; Manitoba Energy and Mines, Geological Services, Open File Report OF98-9, 26 p.

Syme, E.C., Bailes, A.H., Stern, R.A. and Lucas, S.B. 1996: Geochemical characteristics of 1.9 Ga tectonostratigraphic assemblages and tectonic setting of massive sulphide deposits in the Paleoproterozoic Flin Flon belt, Canada; *in* Trace Element Geochemistry of Volcanic Rocks: Applications for Massive Sulphide Exploration, D.A. Wyman (ed.), Geological Association of Canada, Short Course Notes, v. 12, p. 279–327.

Syme, E.C., Lucas, S.B., Zwanzig, H.V., Bailes, A.H., Ashton, K.E. and Haidl, F.M. 1998: Geology, NATMAP Shield Margin Project area, Flin Flon Belt, Manitoba-Saskatchewan; Manitoba Energy and Mines, Geological Services, Map AFP A-98-2, scale 1:100 000.

Winchester, J.A. and Floyd, P.A. 1977: Geochemical discrimination of different magma series and their differentiation products using immobile elements; Chemical Geology, v. 20, p. 326–336.

Wood, D.A. 1980: The application of a Th-Hf-Ta diagram to problems of tectonomagmatic classification and to establishing the nature of crustal contamination of basaltic lavas of the British Tertiary Volcanic Province; Earth and Planetary Science Letters, v. 50, p. 11–30.